Lightning Impulse and AC Breakdown Characteristics of SF6 and its Alternatives

DOI:
10.1109/ICD53806.2022.9863486

Document Version
Accepted author manuscript

Citation for published version (APA):
Ranjan, P., Han, Q., Bahdad, F. O., Alabani, A., Chen, L., Iddrissu, I., & Zel, L. V. D. (2022). Lightning Impulse and AC Breakdown Characteristics of SF6 and its Alternatives. In *2022 IEEE 4th International Conference on Dielectrics* (pp. 672-675) https://doi.org/10.1109/ICD53806.2022.9863486

Published in:
2022 IEEE 4th International Conference on Dielectrics

Lightning Impulse and AC Breakdown Characteristics of SF_6 and its Alternatives

P. Ranjan[1], Q. Han[1], F. O. Bahdad[1], A. Alabani[1], L. Chen[1]*, I. Iddrissu[2], and L. van der Zel[3]
[1]Department of Electrical and Electronic Engineering, The University of Manchester, Manchester, M13 9PL, UK
[2]National Grid Electricity Transmission plc, 1-3 Strand, London, WC2N 5EH, UK
[3]Power Delivery and Utilization, Electric Power Research Institute, NC, 28262-7097, USA
*lujia.chen@manchester.ac.uk

Abstract- **SF_6 alternatives with significantly lower environmental impact have been extensively researched. This paper investigates two electrode configurations and test pressures to mimic the conditions as found in MV/HV equipment to systematically compare the breakdown performance of SF_6, $C_3H_2F_4$ and a mixture of 30% CF_3I / 70% CO_2 under AC and LI stresses. SF_6 possesses comparatively better breakdown performance than the other alternatives investigated in this study. $C_3H_2F_4$ shows "first breakdown" behavior and only the stable data series is considered for evaluation of 50% breakdown voltage, U_{50}. The lower boiling points of $C_3H_2F_4$ and CF_3I limit its potential application to medium-voltage equipment with a low operating pressure. Due to pyrolysis, there is formation of soot and iodine post-breakdown in $C_3H_2F_4$ and 30% CF_3I / 70% CO_2 respectively. This will reduce their dielectric performance and could pose health hazard to maintenance personnel.**

I. INTRODUCTION

High global warming potential (GWP) of SF_6 and the drive towards Net Zero have resulted in an increasing interest for insulating gases with low GWP. Different studies were carried out to phase out the usage of SF_6 either as a newbuild or a retro-fill solution [1] in a functional SF_6 equipment.

CIGRE WG D1.51 [2] studied the feasibility of natural origin gases such as air and CO_2. However, the comparatively low dielectric strength of these gases, about one third of SF_6, makes it a less viable option especially for high-voltage (HV) equipment. Most of the new alternatives have the drawback of high boiling point, which can be mitigated through the use of CO_2 or N_2 as a buffer gas to avoid liquefaction.

3M^{TM} developed Novec^{TM} insulating gases, namely, C_3F_7CN (C4-FN or Novec^{TM} 4710) and $C_5F_{10}O$ (C5-FK or Novec^{TM} 5110) which have been widely researched with newbuild equipment installed in the network [3]. $C_3H_2F_4$, also known as HFO1234ze(E) is researched as a potential SF_6 alternatives but generates soot formation [4] due to pyrolysis under electrical discharges. CF_3I is another candidate investigated as a mixture with CO_2 or N_2 [5]. The aforementioned studies provide a quantitative study on individual gases or mixtures but do not compare these gases under identical experimental conditions.

As part of CIGRE WG D1.67 [6], a round-robin investigation was carried out on the insulating properties of different alternatives such as $C_3H_2F_4$, CF_3I, C_3F_7CN, $C_5F_{10}O$ against SF_6. Researchers at The University of Manchester focused on breakdown performance of $C_3H_2F_4$ and 30% CF_3I / 70% CO_2 against SF_6 under AC and LI voltage stresses. Experimental setup and the breakdown results are detailed in Sections II and III respectively. The visual inspection of gas degradation post-breakdown is discussed in Section IV.

II. EXPERIMENTAL SETUP

A hemispherical-rod to plane configuration was used with a gap of 10 mm and a hemispherical rod diameter of 7 mm. This is to mimic the field uniformity of contacts in 11 kV ring main unit. A sphere to plane configuration with a gap of 15 mm and a sphere diameter of 40 mm was used to represent the field uniformity in HV equipment. The field utilization factor, *f*, of the hemispherical-rod to plane and sphere to plane electrode configurations is 0.297 and 0.628 respectively. The total height of the roughness (R_t) of the HV electrodes, i.e., hemispherical-rod and sphere, were 50 µm and 20 µm, respectively. Gas pressures of 1.3 and 6 bar were tested to mimic the typical operating pressures of medium-voltage (MV) and HV gas-insulated equipment, respectively. All pressures in this paper are absolute pressure in bar. Table I shows different gases tested with their corresponding test parameters. Table II shows the dew temperature of tested gases with the corresponding critical pressure reduced electric field strength (E/p in kV/mm/bar). $C_3H_2F_4$ liquifies at room temperature under 6 bar and its dielectric performance was evaluated at 1.3 bar only.

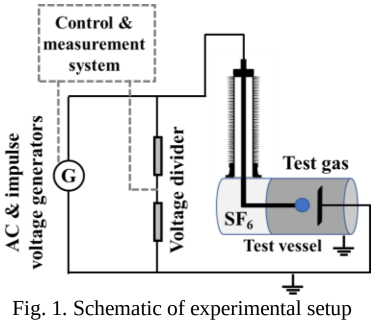

Fig. 1. Schematic of experimental setup

Spacers of 10 and 15 mm thickness were fabricated to accurately set the inter-electrode gap spacing prior to any experiment. A stainless-steel pressure vessel was connected to the HIGHVOLT 800 kV AC test set or BHT 800 kV impulse generator as shown in Fig. 1. The voltage dividers were used to measure the breakdown voltages. The bushing side of the vessel is always filled with SF_6. Vessel was filled with the test gas after (a) vacuuming, (b) filling CO_2 to remove residual moisture, and (c) re-vacuuming the vessel down to 1 mbar. In the case of a single test gas, a direct filling procedure is adopted. For gas mixture, the manometric method is used where 30% of the total required pressure was first filled with CF_3I and then topped up with CO_2.

TABLE I EXPERIMENTAL PARAMETERS

Configuration	*f*	Gas type	Voltage stress	Pressure (bar)
Hemispherical-rod-to-plane	0.297	SF_6, $C_3H_2F_4$, 30% CF_3I / 70% CO_2	±LI, AC	1.3
Sphere-to-plane	0.628	SF_6, 30% CF_3I / 70% CO_2	±LI, AC	6

TABLE II CALCULATED DEW POINT AND E/p OF THE TESTED GASES

Test gas	Dew temperature (°C)		E/p*
	1.3 bar	6 bar	(kV/mm/bar)
SF_6	-62.6	-24.6	8.9
$C_3H_2F_4$	-14.1	30.8	7.1
30% CF_3I / 70% CO_2	-41.6	-4.4	5.5

*Values for 1 bar pressure under uniform electric field

Procedures detailed in [7] were followed for the tests in this paper with a time interval of 2 minutes between successive voltage applications. Each test series consists of 100 voltage applications. For LI tests, up-and-down method with a step voltage of 2.5% of the first breakdown was used to evaluate U_{50}, and standard deviation, σ using equations provided in [8]. For AC tests, a continuous rising method was used with a fast ramp rate of 5 kV/s for the first 40% and a slow ramp rate of 0.5 kV/s for the last 60% of the prospective breakdown voltage. The mean value of the 100 breakdowns was designated as U_{50} for AC tests.

III. RESULTS AND DISCUSSION

Fig. 2 shows the applied voltage sequence for all three gases using the hemispherical-rod to plane electrode. For $C_3H_2F_4$, the data trend can be seen to have less variation when compared to that for SF_6 and 30% CF_3I / 70% CO_2, especially under +LI. This is due to the soot formation after the first breakdown [4] occurred for both LI polarities. The first breakdown behavior for $C_3H_2F_4$ is illustrated in Fig. 3 where the data series is more stable after the first withstand following the first breakdown and multiple voltage collapses all chopped on the front. This unique first breakdown for $C_3H_2F_4$ was prominent under +LI and can be double of the U_{50} value. For the calculation of U_{50} and σ of $C_3H_2F_4$, the final stabilized 100 voltage applications were used as shown in Fig. 2 and as highlighted in yellow in Fig. 3.

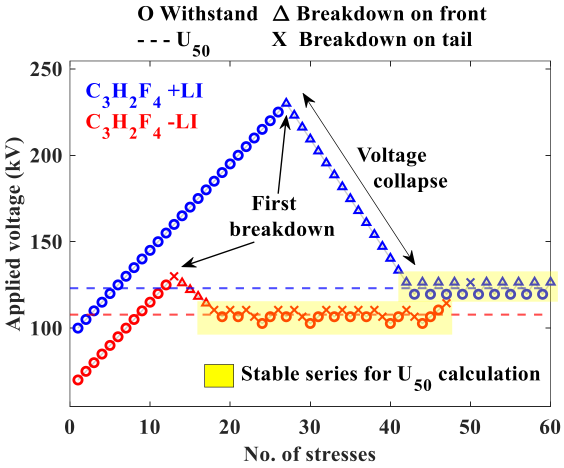

Fig. 3. Examples of LI test sequence for $C_3H_2F_4$ using 25 mm dia. hemisphere to plane configuration with a gap of 10 mm and under a pressure of 2 bar [4]

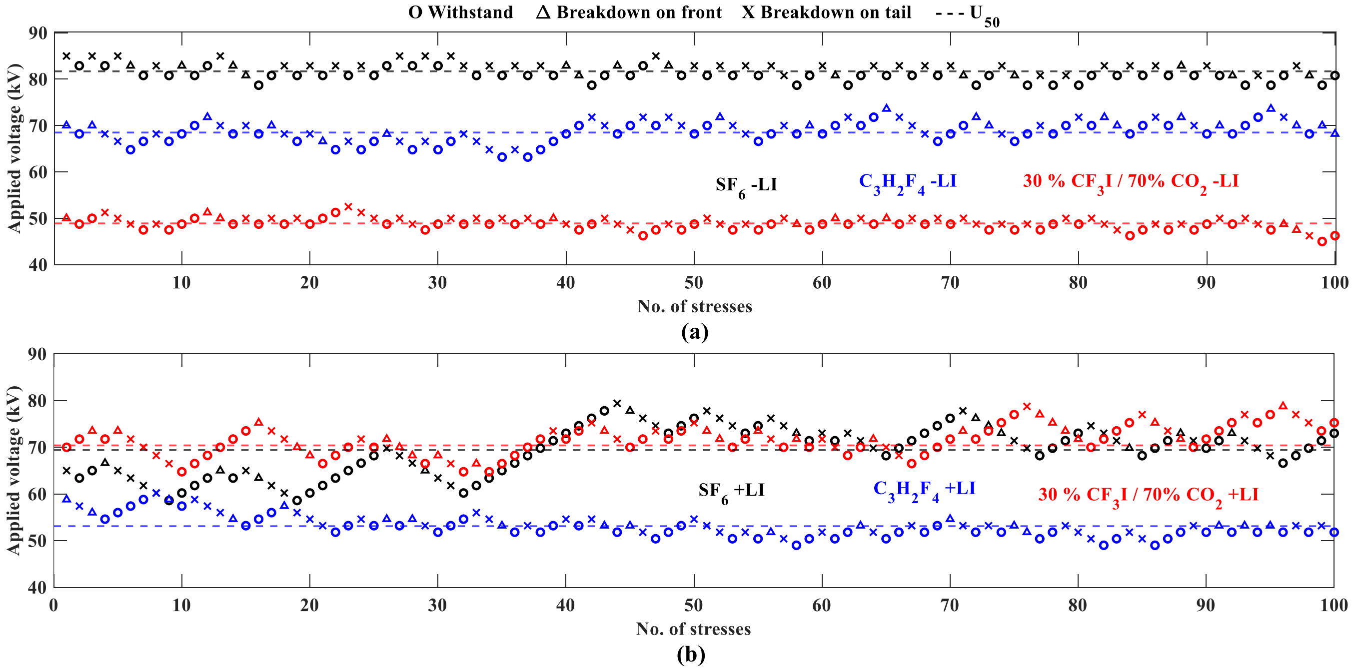

Fig. 2. LI test sequences for different gases under (a) –LI and (b) +LI, using a hemispherical-rod to plane configuration with a fixed gap of 10 mm and a pressure of 1.3 bar

For –LI, the data sequence is comparatively stable with lower σ than +LI as shown in Fig. 4. For $C_3H_2F_4$ and SF_6, higher U_{50} values were observed for –LI on account of a positively headed space charge at the HV electrode which reduces the electric field [4]. However, 30% CF_3I / 70% CO_2 exhibit higher U_{50} in +LI than –LI. Similar polarity effect was reported in [5] using coaxial geometry. The opposite polarity effect was observed when the field is non-uniform and tested at a comparable pressure [9].

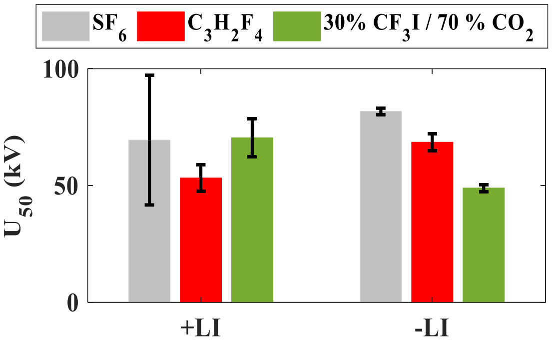

Fig. 4. Plot of U_{50} and σ for different gases using a hemispherical-rod to plane configuration with a gap of 10 mm and under a pressure of 1.3 bar

Impulse Ratio Calculations

Impulse ratio is defined as the ratio of withstand/breakdown LI voltage to the corresponding AC_{peak} withstand/breakdown voltage. This is an engineering value that helps with design margin consideration for gas insulated systems [2] to fulfill the specified withstand voltages. The highlighted “yellow” region in Fig. 5 shows the limits specified in IEC 62271-1 [10]. Data points show the impulse ratios from the experimentally obtained values as depicted in Table III.

When the experimental obtained ratios are higher than the IEC defined impulse ratio range, the insulation system design is dominated by AC. Vice versa, LI voltage is more important if the experimentally obtained ratio is below the IEC impulse ratio range. For 1.3 bar, –LI values are within the IEC impulse ratio limit while for +LI, it is lower except that of 30% CF_3I / 70% CO_2. For 6 bar, all the experimental ratios are lower than that of IEC ones. These values indicate that the insulation system design for MV (1.3 bar) or HV (6 bar) applications will be decided by LI withstand tests for the tested gases. This also agrees with [2], where dry air, N_2, CO_2 and SF_6 insulated systems until 7 bar, are dominated by LI voltages.

TABLE III. U_{50} FOR TESTS OBTAINED IN THE PRESENT WORK

Hemispherical-rod to plane / 10 mm / 1.3 bar					
Test gas	+LI (kV)	–LI (kV)	AC_{peak} (kV)	Impulse Ratio	
				+LI	–LI
SF_6	69.4	81.7	52.3	1.33	1.56
$C_3H_2F_4$	53.1	68.5	47.9	1.11	1.43
30% CF_3I / 70% CO_2	70.4	48.9	29.9	2.35	1.64
Sphere to plane / 15 mm / 6 bar					
SF_6	489.6	408.5	368.3	1.33	1.11
30% CF_3I / 70% CO_2	332.7	279.3	271.4	1.23	1.03

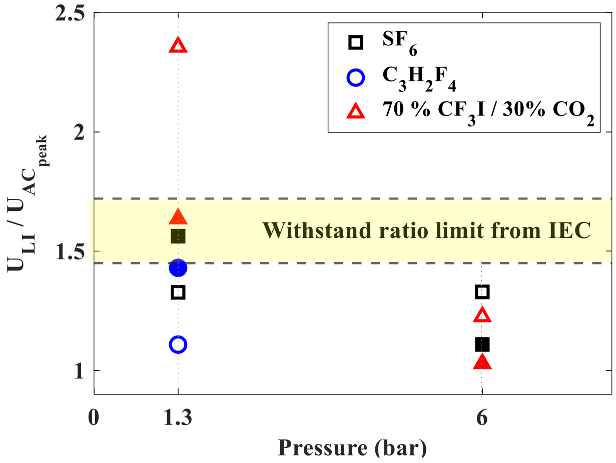

Fig. 5. Ratio of U_{50} under LI and AC voltage stresses for the investigated test conditions in the present work (unfilled markers: +LI; filled markers: –LI)

IV. DECOMPOSITION AFTER EXTENSIVE AC BREAKDOWNS

For SF_6, there was no obvious decomposition observed unlike $C_3H_2F_4$ and 30% CF_3I / 70% CO_2. The byproducts after the tests and during the cleaning of electrodes/vessel were photographed as detailed in subsequent paragraphs.

Soot Formation in $C_3H_2F_4$

Fig. 6 shows the photographs of test electrodes after 100 AC breakdowns using $C_3H_2F_4$ under 1.3 bar. The dark colored soot deposited on the electrodes was identified as fluorinated carbon due to pyrolysis. Experiments carried out in [4] showed soot formation which did not appear to react with the metal electrode surface and can be easily wiped off. The formation of soot can be minimized with the addition of O_2. Considering the boiling point of $C_3H_2F_4$, it can be used as an insulation medium in non-switching MV equipment, but one must take into account the soot formation and its potential adverse effect on insulation performance.

(a) (b)

Fig. 6. Photos taken after 100 AC breakdown of $C_3H_2F_4$ under 1.3 bar: (a) plane electrode and (b) hemispherical-rod electrode

Iodine Formation in CF_3I

In the case of 30% CF_3I / 70% CO_2, extended AC breakdowns under 6 bar caused the colorless gas to turn orange/red which was not observed in other test gases. Note that the discharge energy of the AC generator used was ~10 times higher than the LI generator used in this study. For 30% CF_3I / 70% CO_2 under 6 bar, the colorless CF_3I gas in the test vessel changed to orange/red color as shown in Fig. 7(a). It is the characteristic color of iodine vapor and was reported in [11] after electrical discharges. The electrodes shortly after opening the test vessel are shown in Figs. 7(b) and 7(c). The plane electrode showed different colors of red, brown, and purple. Sphere and plane electrodes appear moist when first taken out of the vessel. This may be due to hygroscopic nature of iodide salts or the degradation product on the surface of the electrode reacting with moisture in the open-air.

The electrodes and test chamber were cleaned with the isopropanol and cleaning paper. Different colors were visually observed on the cleaning paper. The yellow color on the paper may be due to the free iodine in the test vessel. The red/purple color on the plane electrode and the cleaning paper indicates the precipitation of iodine on the electrode surface. This was confirmed by Fig. 7(d) where brown colored solid precipitates can be seen on the sphere electrode after being exposed to open-air for several days.

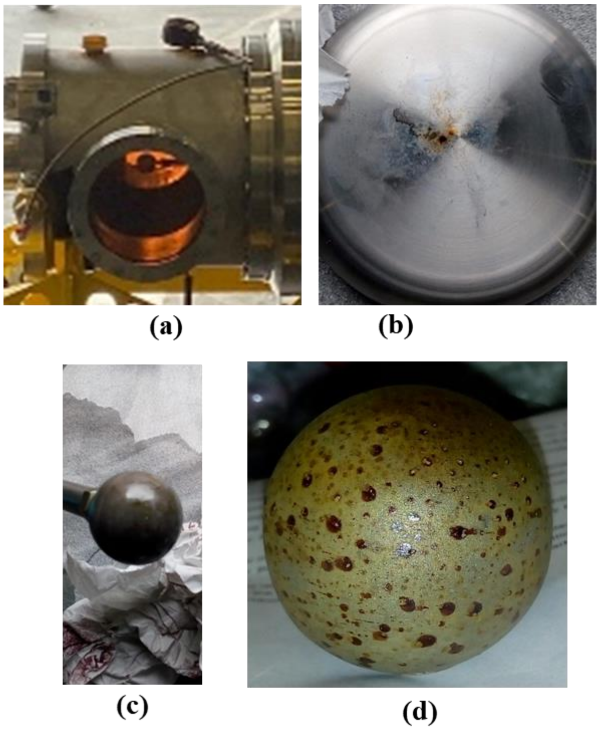

Fig. 7. Photos taken after 100 AC breakdowns of 30% CF_3I / 70% CO_2 under 6 bar: (a) test chamber with orange/red colored gas, (b) plane electrode, (c) 40 mm sphere electrode; (d) different colored deposits found on the cleaning papers and (e) sphere electrode after several days in open-air environment

Iodine decomposition of 30% CF_3I / 70% CO_2 mixture poses considerable challenge for its use in MV/HV equipment. The gas handling for this two-component gas needs to be carried out with care avoiding ingress of moisture and/or O_2. The chamber must be cleaned with appropriate personal protective equipment such as hand gloves and full-face respirator, and preferably to be carried out in a well-ventilated area.

V. CONCLUSIONS

For breakdown performance evaluation under LI tests, a stable data series should be assessed after the pre-conditioning. For all three tested gases, –LI test data had comparatively less voltage levels in up-and-down test than +LI. The U_{50} values will vary depending on the gas medium, field configurations and especially the polarity of applied voltage. This indicates that gases must be evaluated for both polarities to determine the insulation system design parameter.

The comparatively higher boiling point limits the application of $C_3H_2F_4$ and CF_3I to MV non-switching equipment. The formation of by-products such as fluorinated carbon soot and iodine post-breakdowns present operational risk of surface flashover occurrence at significantly reduced voltage withstand level due to solid precipitation along the insulator.

ACKNOWLEDGMENT

This work was supported by Electric Power Research Institute (EPRI), USA. The authors also acknowledge EPSRC for support through "High Voltage Test Systems for Electricity Network Research" [grant number EP/P030343/1].

For the purpose of open access, the author has applied a CC BY public copyright license to any Author Accepted Manuscript version arising from this submission.

REFERENCES

[1] L. Loizou, L. Chen, Q. Liu, I. Cotton, M. Waldron and J. Owens, "Technical Viability of Retro-Filling C_3F_7CN/CO_2 Gas Mixtures in SF_6-Designed Gas Insulated Lines and Busbars at Transmission Voltages," *IEEE Trans. Power Deliv.*, vol. 35, no. 5, pp. 2394-2402, 2020.

[2] WG D1.51, "Dry air, N_2, CO_2, and N_2/SF_6 mixtures for gas-insulated systems," *CIGRE*, Technical Brochure 730, 2018.

[3] J. Owens, A. Xiao, J. Bonk, M. DeLorme, and A. Zhang, "Recent Development of Two Alternative Gases to SF_6 for High Voltage Electrical Power Applications," *Energies*, vol. 14, no. 16, pp. 1-4, 2021.

[4] P. Ranjan, L. Chen, A. Alabani, F. Bahdad, I. Cotton, and L. van der Zel, "Anomalous First Breakdown Behavior of HFO1234ze(E)," *IEEE Trans. Dielectr. Electr. Insul.*, vol. 28, no. 5, pp. 1620-1627, 2021.

[5] L. Chen, P. Widger, M. S. Kamarudin, H. Grirffiths and A. Haddad, "CF_3I Gas Mixturess: Breakdown Characteristics and Potential for Electrical Insulation," *IEEE Trans. Power Deliv.*, vol. 32, no. 2, pp. 1089-1097, 2017.

[6] WG D1.67, "Electric performance of new non-SF_6 gases and gas mixtures for gas-insulated systems," *CIGRE*, Technical Brochure 849, 2021.

[7] *High-voltage test techniques – Part 1: General definitions and test requirements*, IEC 60060-1:2010, 2010.

[8] W. Hauschild and W. Mosch, *Statistical Techniques for High-Voltage Engineering*, London, United Kingdom, IET, 1992.

[9] L. Chen, M. S. Kamarudin, H. Griffiths, and A. Haddad, "Breakdown of CF_3I Gas and its Mixtures under Lightning Impulse in Coaxial-GIL Geometry," *IEEE Trans. Dielectr. Electr. Insul.*, vol. 23, no. 4, pp. 1959-1967, 2016.

[10] *High-voltage switchgear and controlgear – Part 1: Common specifications for alternating current switchgear and controlgear*, IEC 62271-1:2017, 2017.

[11] S. Xiao, Y. Li, X. Zhang, J. Tang, S. Tian, and Z. Deng, "Formation mechanism of CF_3I discharge components and effect of oxygen on decomposition," *J. Phys. D. Appl. Phys.*, vol. 50, pp. 155601 (1-12), 2017.